

# Temporal Dynamics of Normalization Reweighting

Daniel H. Baker, Daniela Marinova, Richard Aveyard, Lydia J. Hargreaves, Alice Renton,  
Ruby Castellani, Phoebe Hall, Miriam Harmens, Georgia Holroyd, Beth Nicholson,  
Emily L. Williams, Hannah M. Hobson & Alex R. Wade

Department of Psychology, University of York, UK

## 1 Abstract

For decades, neural suppression in early visual cortex has been thought to be fixed. But recent work has challenged this assumption by showing that suppression can be *reweighted* based on recent history; when pairs of stimuli are repeatedly presented together, suppression between them strengthens. Here we investigate the temporal dynamics of this process using a steady-state visual evoked potential (SSVEP) paradigm that provides a time-resolved, direct index of suppression between pairs of stimuli flickering at different frequencies (5 and 7Hz). Our initial analysis of an existing EEG dataset (N=100) indicated that suppression increases substantially during the first 2-5 seconds of stimulus presentation (with some variation across stimulation frequency). We then collected new EEG data (N=100) replicating this finding for both monocular and dichoptic mask arrangements in a preregistered study designed to measure reweighting. A third experiment (N=20) used source localized MEG, and found that these effects are apparent in primary visual cortex (V1), consistent with results from neurophysiological work. Because long-standing theories propose inhibition/excitation differences in autism, we also compared reweighting between individuals with high vs low autistic traits, and with and without an autism diagnosis, across our 3 data sets (total N=220). We find no compelling differences in reweighting that are associated with autism. Our results support the normalization reweighting model, and indicate that for prolonged stimulation, increases in suppression occur on the order of 2-5 seconds after stimulus onset.

## 18 2 Introduction

Suppressive interactions between neurons are ubiquitous in the nervous system, with normalization considered a canonical neuronal computation (Carandini and Heeger, 2011). Yet for decades the strength of suppression was treated as fixed, due to the observation that adapting to one stimulus does not decrease its suppressive potency (Foley and Chen, 1997; Freeman et al., 2002). This orthodoxy has been challenged by a series of innovative studies showing that normalization can be ‘reweighted’ by recent history (Aschner et al., 2018; Westrick et al., 2016; Yiltiz et al., 2020). When pairs of stimuli are repeatedly presented together, their neural representations come to suppress each other more strongly. Far from being fixed, normalization is therefore a dynamic process that is continuously updated by the sensory environment. Our objectives were to measure the timecourse of these changes non-invasively in the human brain, compare them across distinct suppressive pathways, and determine whether they differ as a function of autistic traits.

Plastic changes within the visual system occur over multiple timescales (see Webster, 2015 for a recent review). Cortical forms of adaptation to cues such as stimulus contrast (Blakemore and Campbell, 1969), orientation (Gibson and Radner, 1937) and motion (Mather et al., 2008) can be observed within a few seconds, but also build up over durations on the order of minutes (Greenlee et al., 1991). Other types of adaptation have been identified where changes occur over longer time periods, such as several hours (Kwon et al., 2009) or days (Haak et al., 2014). Previous normalization reweighting studies involved adapting sequences of around 40 – 60s (Aschner et al., 2018; Yiltiz et al., 2020), but in principle reweighting might occur faster than this, consistent with other types of contrast adaptation.

37 Multiple suppressive pathways have been identified in the visual system, including between stimuli differing  
38 in orientation (Foley, 1994; Heeger, 1992), eye-of-origin (Legge, 1979; Sengpiel and Blakemore, 1994) and  
39 spatial position (Cannon and Fullenkamp, 1991; Petrov, 2005). At present there is evidence of normalization  
40 reweighting between stimuli with orthogonal orientations (Aschner et al., 2018), and adjacent spatial positions  
41 (Yiltiz et al., 2020). We anticipated that interocular suppression should also be subject to reweighting, but  
42 that there might be differences in the dynamics across suppressive pathways (Li et al., 2005; e.g. Meese  
43 and Baker, 2009; Sengpiel and Vorobyov, 2005). Comparing monocular and dichoptic suppression permits  
44 any contribution of early pre-cortical factors to be isolated. This is because interocular suppression impacts  
45 in primary visual cortex, and bypasses any retinal and subcortical stages of processing that contribute to  
46 monocular suppression (Li et al., 2005).

47 Atypical sensory experience, including hypersensitivity to loud sounds, bright lights and strong odours or  
48 flavours, is widely reported by individuals on the autism spectrum (MacLennan et al., 2022; Simmons et al.,  
49 2009), but the causal mechanisms remain unclear. Fundamental measures of sensitivity including visual acuity  
50 (Tavassoli et al., 2011), contrast sensitivity (Koh et al., 2010), and audiometric performance (Rosenhall et al.,  
51 1999) are not consistently different from neurotypical controls. Theoretical accounts of sensory differences  
52 in autism have proposed that the balance of inhibition and excitation may be disrupted (Rosenberg et al.,  
53 2015; Rubenstein and Merzenich, 2003), yet the evidence is currently inconclusive (Sandhu et al., 2020; e.g.  
54 Schallmo et al., 2020; Van de Cruys et al., 2018). Our recent work identified an autism-related difference  
55 using steady-state EEG (Vilidaite et al., 2018), in which nonlinear (second harmonic) responses were weaker,  
56 implicating atypical suppression in autism.

57 Here we perform a time-course analysis of a previously published data set, and report two novel pre-registered  
58 experiments using EEG and MEG. Our data show that suppression increases substantially during the first 2-5  
59 seconds following stimulus onset, for both monocular and dichoptic masks. Source localisation of MEG data  
60 indicate that the reweighting is present as early as primary visual cortex (V1). We also hypothesised that  
61 normalization reweighting might differ as a function of autistic traits, but did not find convincing support for  
62 this hypothesis.

### 63 **3 Materials and Methods**

#### 64 **3.1 Participants**

65 Experiment 1 was completed by 100 adult participants (32 male, 68 female; mean age 21.9) in early 2015,  
66 and first reported by Vilidaite et al. (2018). Here we reanalysed the dataset, and report the results of  
67 masking conditions not previously published. Experiment 2 was completed by 100 adult participants (23  
68 male, 74 female, 3 other/not stated; mean age 22.1) in early 2022. Experiment 3 was completed by 10  
69 adults (2 male, 8 female) with a clinical diagnosis of autism, and 10 control participants who were closely  
70 matched for age (means of 21.8 and 22,  $t = 0.18$ ,  $df = 18$ ,  $p = 0.86$ ) and exactly matched for gender.  
71 Procedures in Experiments 1 and 2 were approved by the ethics committee of the Department of Psychology  
72 at the University of York. Procedures for Experiment 3 were approved by the ethics committee of the York  
73 Neuroimaging Centre. All participants provided written informed consent, and procedures were consistent  
74 with the Declaration of Helsinki.

#### 75 **3.2 Apparatus and stimuli**

76 In Experiments 1 and 2, stimuli were presented using a ViewPixx 3D LCD display device (VPixx Technologies,  
77 Canada) with a resolution of  $1920 \times 1080$  pixels and a refresh rate of 120Hz. The display was gamma  
78 corrected using a Minolta LS110 photometer. In Experiment 2, participants wore active stereo shutter glasses  
79 (NVidia 3D Vision 2) that were synchronised with the display using an infra-red signal. EEG data were  
80 collected using a 64-channel Waveguard cap, and were amplified and digitised at 1000Hz using an ANT  
81 Neuroscan system. Electrode impedance was maintained below  $5k\Omega$ , and referenced to a whole-head average.  
82 In Experiment 3, stimuli were presented using a ProPixx DLP projector (VPixx Technologies) running at  
83 120Hz. Stereo presentation was enabled using a circular polariser that was synchronised with the projector

refresh, and participants wore passive polarised glasses during the experiment. DLP projectors are perfectly linear, so gamma correction was not required. Data were acquired using a refurbished 248-channel 4D Neuroimaging Magnes 3600 MEG scanner, recording at 1001Hz. Participant head shape was digitised using a Polhemus Fastrak device, and head position was recorded at the start and end of each block by passing current through 5 position coils placed at fiducial points on the head. We also obtained structural MRI scans using a 3 Tesla Siemens Magnetom Prisma scanner to aid in source localisation. Two participants were not available for MRI scans, so we used the MNI ICBM152 template brain (Fonov et al., 2011) for these individuals.

Stimuli were patches of sine wave grating with a diameter of 2 degrees, flickering sinusoidally (on/off flicker) at either 5Hz or 7Hz. In Experiment 1 the gratings had a spatial frequency of 0.5c/deg, and in Experiments 2 & 3 this was increased to 2c/deg. A symmetrical array of 36 individual patches tiled the display. In Experiment 1 the patch orientation was randomly selected on each trial, and all patches had the same orientation. In Experiments 2 & 3 each patch had a random orientation, which was intended to prevent any sequential effects between trials with similar orientations. The central patch was omitted and replaced by a fixation marker constructed from randomly overlaid squares. During each experiment, the fixation marker could be resampled on each trial with a probability of 0.5. Participants were instructed to monitor the fixation marker and count the number of times it changed throughout the experiment. This was intended to maintain attention towards the display and keep participants occupied.

Participants also completed either the short AQ (Hoekstra et al., 2011) in Experiment 1, or the full AQ (Baron-Cohen et al., 2001) in Experiments 2 and 3. For comparison across experiments, we rescaled the short AQ to the same range as the full AQ (0-50). In Experiments 2 and 3, the sensory perception quotient (SPQ) questionnaire (Tavassoli et al., 2014) was also completed.

### 3.3 Experimental design and statistical analysis

In Experiment 1, target stimuli flickering at 7Hz were presented at a range of contrasts (1 - 64%). In half of the conditions a superimposed orthogonal mask of 32% contrast was presented simultaneously, flickering at 5Hz. Stimuli were displayed for trials of 11 seconds, with a 3 second inter-trial interval. The experiment consisted of 4 blocks of trials, each lasting around 10 minutes, and resulting in 8 repetitions of each condition. Participants viewed the display from 57cm, were comfortably seated in an upright position, and were able to rest between blocks. Low latency 8-bit digital triggers transmitted the trial onset and condition information directly to the EEG amplifier.

The procedure for Experiment 2 was very similar, except that participants also wore stereo shutter glasses during the experiment. There were four conditions: (i) monocular presentation of a 5Hz stimulus of 48% contrast, (ii) monocular presentation of a 7Hz stimulus of 48% contrast, (iii) monocular presentation of both stimuli superimposed at right angles, and (iv) dichoptic presentation of both stimuli at right angles (i.e. one stimulus to the left eye, one to the right eye). Eye of presentation was pseudo-randomised to ensure equal numbers of left-eye and right-eye presentations. The trial duration was 6 seconds, with a 3 second inter-trial interval. Participants completed 3 blocks, each lasting around 10 minutes, resulting in a total of 48 repetitions of each condition. Experiment 3 was identical, except that the projector screen was viewed from a distance of 85cm.

EEG data from Experiments 1 and 2 were first imported into Matlab using components of the EEGLab toolbox (Delorme and Makeig, 2004), and converted into a compressed ASCII format. Primary data analysis was then conducted using a bespoke *R* script. In brief, we epoched each trial and extracted the average timecourse across four occipital electrodes (*Oz*, *POz*, *O1* and *O2*), and then calculated the Fourier transform of this average waveform. We excluded trials for which the Mahalanobis distance of the complex Fourier components exceeded 3 (for details see Baker, 2021). This resulted in 0.25% of trials being excluded for Experiment 1, and 4.51% of trials for Experiment 2. Next we averaged the waveforms across all remaining trials, and calculated the Fourier transform in a 1-second sliding window to generate timecourses for each participant. We divided the timecourse for the target-only condition by the timecourse for the target + mask condition to produce a suppression ratio. These were then converted to logarithmic (dB) units for averaging, calculation of standard errors, and statistical comparisons. For display purposes we smoothed the timecourses

134 using a cubic spline function, however all statistical comparisons used the unsmoothed data.

135 For Experiment 3, we performed source localisation using a linearly constrained minimum variance (LCMV)  
136 beamformer algorithm, implemented in Brainstorm (Tadel et al., 2011). Structural MRI scans were processed  
137 using Freesurfer (Dale et al., 1999) to generate a 3D mesh of the head and brain, and we calculated source  
138 weights for each block with reference to a 5-minute empty room recording, usually recorded on the day of  
139 the experiment. The matrix of source weights for each block was used in a custom Matlab script to extract  
140 signals from V1, identified using the probabilistic maps of Wang et al. (2015). These signals were then  
141 imported into R for the main analysis, which was consistent with the EEG analysis described above. The  
142 outlier rejection procedure excluded 2.47% of trials for Experiment 3.

143 To make comparisons between groups of participants across time, we used a non-parametric cluster correction  
144 technique (Maris and Oostenveld, 2007) based on t-tests. Clusters were identified as temporally adjacent  
145 observations that were all statistically significant, and a summed t-value was calculated for each cluster.  
146 A null distribution was then generated by randomising group membership and recalculating the summed  
147 t-value for the largest cluster, and repeating this procedure 1000 times. Clusters were considered significant if  
148 they fell outside of the 95% confidence limits of the null distribution. We adapted this approach to test for  
149 significantly increasing suppression by conducting one-way t-tests between time points separated by 1000ms,  
150 and repeating the cluster correction procedure as described above.

### 151 3.4 Preregistration, data and code accessibility

152 Following a preliminary analysis of the data from Experiment 1, we preregistered our hypotheses and analysis  
153 plan for Experiments 2 and 3 on the Open Science Framework website. The preregistration document,  
154 along with raw and processed data, and analysis scripts, are publicly available at the project repository:  
155 <https://osf.io/ab3yv/>

## 156 4 Results

157 We began by reanalysing data from a steady-state visually evoked potential (SSVEP) experiment reported  
158 by Vilidaite et al. (2018). Participants viewed arrays of flickering gratings of varying contrasts. In some  
159 conditions a single grating orientation was present flickering at 7Hz, whereas in other conditions a high  
160 contrast ‘mask’ was added at right angles to the target gratings, and flickering at 5Hz. The left panel of  
161 Figure 1a shows contrast response functions with and without the mask - the presence of the mask reduces  
162 the 7Hz response to the target (blue squares are below the black circles; significant main effect of mask  
163 contrast,  $F(1,99) = 26.52, p < 0.001$ ). Similarly, the right panel of Figure 1a shows that the 5Hz response to  
164 the mask was itself suppressed by the presence of high contrast targets (main effect of target contrast on the  
165 mask response,  $F(2.92,288.63) = 46.77, p < 0.001$ ; note that the data from the masking conditions were not  
166 reported by Vilidaite et al. (2018)). At both frequencies, responses were localised to the occipital pole (see  
167 insets).

168 We then performed a timecourse analysis, in which we analysed each 11-second trial using a sliding 1-second  
169 time window. The top panel of Figure 1c shows the response at the target frequency (7Hz) to a single  
170 stimulus of 32% contrast (black), and the response at 7Hz when the 32% contrast mask is added (blue). For  
171 comparison, a baseline timecourse is also shown (grey), which was the response at 7Hz when a 5Hz stimulus  
172 was shown (therefore controlling for attention, blinking etc.). Analogous responses are shown at three other  
173 frequencies - the mask frequency (5Hz), and the second harmonics of both target and mask frequencies (14Hz,  
174 10Hz), at which strong responses were also found (see spectra in Figure 1b). The reduction in signal strength  
175 when the mask component is added illustrates the masking effect.

176 Taking the ratio of the two timecourses to calculate a masking index reveals that at 7Hz masking increases  
177 steeply during the first two seconds of stimulus presentation, and then plateaus for several seconds (blue  
178 trace in Figure 1d). A similar pattern is observed at 5Hz (red trace in Figure 1d), as well as at the second  
179 harmonics, with some variability in the timecourse across frequencies; for example, at 5Hz suppression peaks  
180 at around 4 seconds. The black trace shows the average masking ratio across all four frequencies, which rises  
181 steeply for just over two seconds and then stays approximately constant until stimulus offset. We conducted

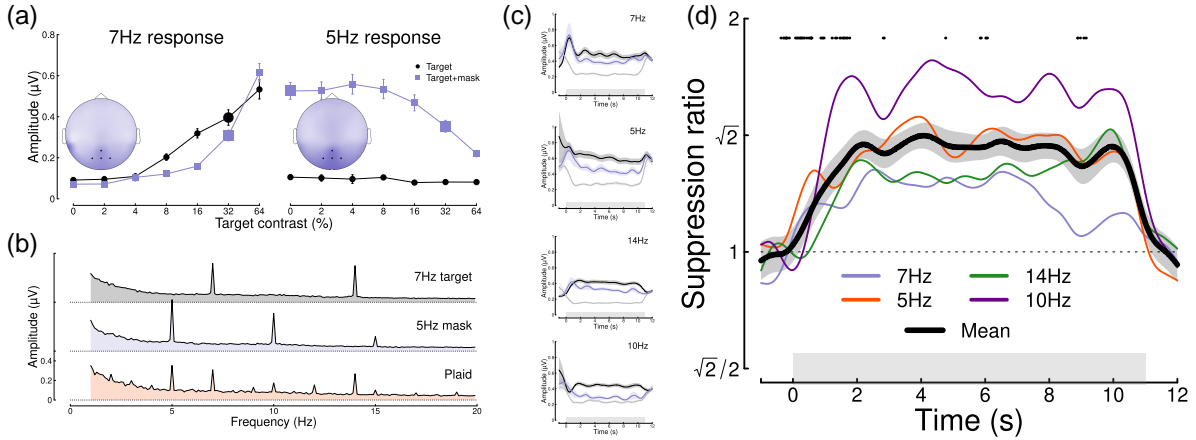


Figure 1: Summary of pilot analysis of data from Vilidiate et al. (2018). Panel (a) shows contrast response functions at the target frequency (7Hz, left) and the mask frequency (5Hz, right). Insets show the distribution of activity across the scalp, with points marking the electrodes over which signals were averaged (Oz, POz, O1 and O2). Panel (b) shows Fourier spectra for the single component stimuli and their combination (plaid). Note the strong second harmonic components at 14Hz and 10Hz. Panel (c) shows timecourses of frequency-locked responses to a single stimulus (black) and the plaid stimulus (blue), compared to baseline (grey). Panel (d) shows the timecourse of suppression at each frequency (7Hz, 5Hz, 14Hz, 10Hz) and their average (black curve). Points around  $y = 1.8$  indicate a significantly increasing ratio. Error bars in panel (a) and shaded regions in panels (c,d) indicate  $\pm 1\text{SE}$  across  $N=100$  participants, and grey rectangles indicate the timing of stimulus presentation. The larger symbols in panel (a) indicate the conditions used for subsequent analyses.

cluster-corrected t-tests between ratios separated by 1000ms, testing for an increase in suppression ratio across time (i.e. a one-sided test). Points at  $y = 1.8$  in Figure 1d indicate time points where the ratio is significantly increasing, and occur mostly during the first 2 seconds of stimulus presentation.

Our initial reanalysis was promising, however the data were noisy despite the large sample size (of  $N=100$ ), because each participant contributed only 8 trials (88 seconds) to each condition. We therefore preregistered two new experiments (see <https://osf.io/4qudc>) to investigate these effects in greater detail. These had a similar overall design to the Vilidaite et al. (2018) study, with some small changes intended to optimise the study (see Methods). The key differences were that we used shorter trials (because there were few changes in the latter part of the trials shown in Figure 1d), and also focussed all trials into a smaller number of conditions, such that each participant contributed 48 repetitions (288 seconds of data) to each of 4 conditions.

Figure 2 summarises the results of our EEG experiment testing a further 100 adult participants. Averaged EEG waveforms showed a strong oscillatory component at each of the two stimulus flicker frequencies (Figure 2a), which slightly lagged the driving signal. Signals were well-isolated in the Fourier domain (Figure 2b), and localised to occipital electrodes. Responses at 7Hz were weaker in the two masking conditions, showing significant changes in response amplitude for both the monocular ( $t = 7.56$ ,  $df = 87$ ,  $p < 0.001$ ) and dichoptic ( $t = 11.35$ ,  $df = 87$ ,  $p < 0.001$ ) masks. Dichoptic masking was significantly stronger than monocular masking ( $t = 7.96$ ,  $df = 87$ ,  $p < 0.001$ ), and a similar pattern was evident at 5Hz.

The timecourse at both flicker frequencies showed an initial onset transient, and was then relatively stable for the 6 seconds of stimulus presentation (Figure 2c,d). The ratio of target only to target + mask conditions increased over time (Figure 2e,f) for both mask types. At 5Hz the increase in masking continued over the first 5 seconds of stimulus presentation (Figure 2e; points at  $y = 0.8$  indicate significantly increasing suppression), whereas at 7Hz the increase occurred primarily during the first second after onset (Figure 2f). These differences across frequency are consistent with the pilot data (see Figure 1d). Both monocular and dichoptic masks produced similar timecourses of suppression. Overall, this second study confirmed that normalization increases during the first few seconds of a steady-state trial, and extends this finding to

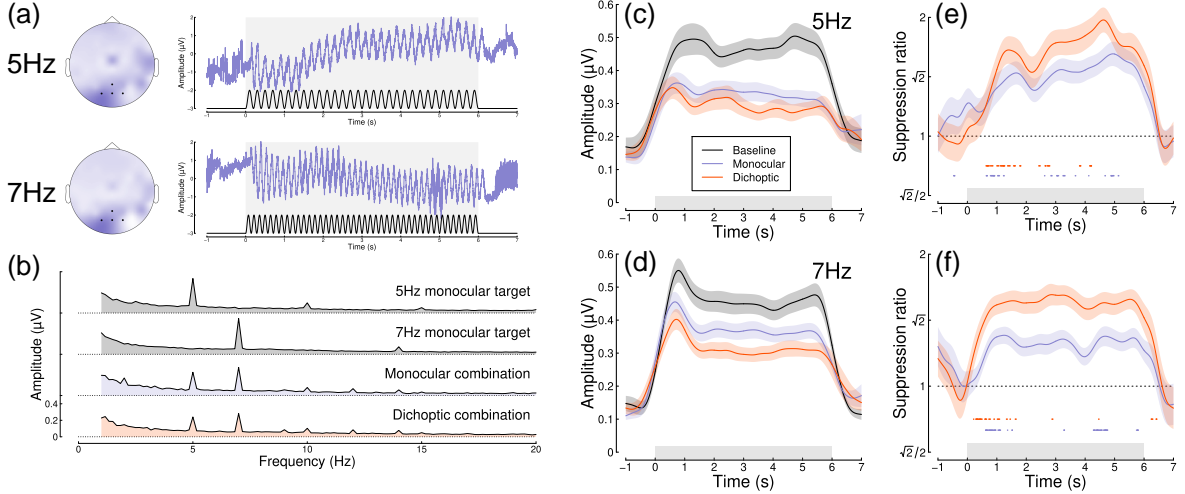


Figure 2: Summary of EEG results for  $N=100$  adult participants. Panel (a) shows scalp topographies and averaged waveforms for 5Hz (top) and 7Hz (bottom) stimuli. The black sine wave trace in each panel illustrates the driving contrast modulation, and black points on the scalp topographies indicate electrodes Oz, O1, O2 and POz. Panel (b) shows the Fourier amplitude spectrum for each condition, with clear peaks at 5Hz and 7Hz. Panels (c,d) show timecourses at each frequency for the baseline condition (black), and the monocular (blue) and dichoptic (red) masking conditions. Panels (e,f) show suppression ratios as a function of time for each mask type, with points around  $y = 0.8$  indicating a significantly increasing ratio. Shaded regions in panels (c-f) span  $\pm 1\text{SE}$  across participants, and light grey rectangles indicate the period of stimulus presentation.

207 dichoptic mask arrangements.

208 Next we repeated the experiment on 20 participants using a 248-channel whole-head cryogenic MEG system.  
 209 Half of the participants had a diagnosis of autism, and the remainder were age- and gender-matched controls.  
 210 Source localisation using a linearly constrained minimum variance (LCMV) beamformer algorithm (Van Veen  
 211 et al., 1997) showed strong localisation of steady-state signals at the occipital pole (see Figure 3a), and in the  
 212 Fourier domain (Figure 3b). Responses from the most responsive V1 vertex showed a similar timecourse to  
 213 those of the EEG experiments at both frequencies (Figure 3c,d), and showed increasing suppression during  
 214 the first few seconds of stimulus presentation (Figure 3e,f). The normalization reweighting effect was again  
 215 clearest at 5Hz, especially for the dichoptic condition (red curve in Figure 3e). This confirms that the  
 216 reweighting effects can occur as early as primary visual cortex, consistent with findings from neurophysiology  
 217 (Aschner et al., 2018). However the data are more variable than for our EEG experiments, and had fewer  
 218 significant clusters, owing to the smaller sample size for this dataset.

219 To investigate whether normalization reweighting effects differ with respect to autistic traits, we then split  
 220 each dataset (averaged across temporal frequency) using median AQ score (for the EEG experiments) or  
 221 according to diagnostic group (autism vs controls) for the MEG data. Figure 4a-c shows distributions of AQ  
 222 scores for each experiment, and indicates for the pilot and EEG data which participants were in the high  
 223 (purple) and low (green) AQ groups. The median AQ scores were 14 for the pilot data, and 18 for the EEG  
 224 data. In the MEG experiment, AQ scores for the autism group (mean 36.1) and the control group (mean  
 225 16.7) were significantly different ( $t = 6.00, df = 14.2, p < 0.001$ ), with minimal overlap (one participant with  
 226 an autism diagnosis had an AQ score marginally lower than the highest AQ scores from the control group).  
 227 These distributions are consistent with previous results for AQ (Baron-Cohen et al., 2001).

228 We compared the timecourse of suppression between groups using a nonparametric cluster correction approach  
 229 (Maris and Oostenveld, 2007) to control the type I error rate. Significant clusters are indicated at  $y = 0.8$  in  
 230 panels d-h of Figure 4. Despite some occasionally significant clusters, there is no clear or consistent difference  
 231 between groups across our three data sets. In particular, none of the significant clusters occur during the first

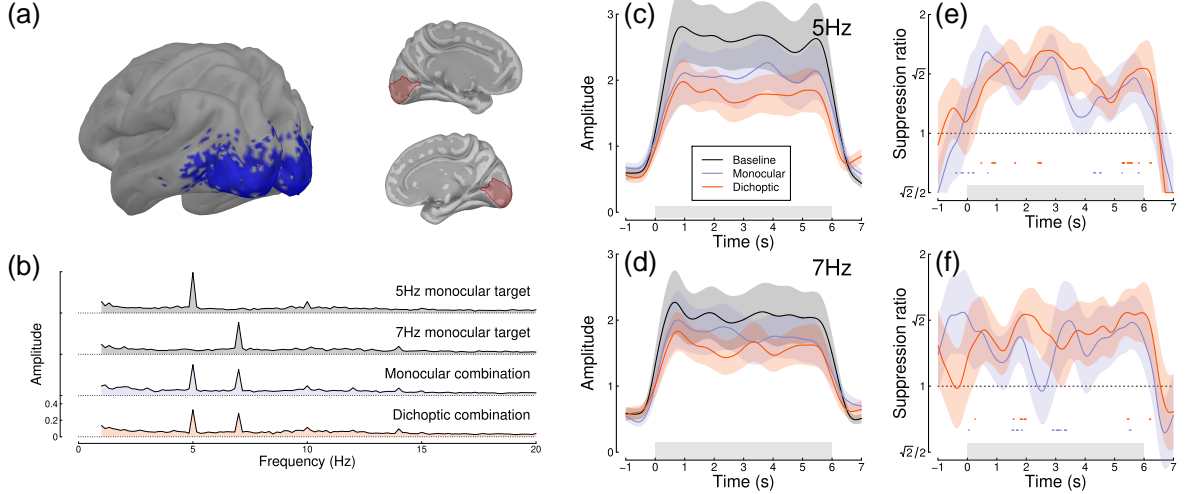


Figure 3: Summary of MEG results for  $N=20$  adults. Panel (a) shows average SSVEP response in source space, thresholded at  $\text{SNR}=2$  (blue, left), and locations of the V1 ROI on the medial surface of both hemispheres (right, red). Panel (b) shows the Fourier spectra for the four experimental conditions, from the most responsive vertex in V1. Panels (c,d) show timecourses at 5Hz and 7Hz, and panels (e,f) show suppression ratios for the monocular and dichoptic conditions at each frequency, with points around  $y = 0.8$  indicating a significantly increasing ratio. Shaded regions in panels (c-f) indicate  $\pm 1\text{SE}$  across participants, and light grey rectangles indicate the period of stimulus presentation.

232 few seconds of stimulus onset, when reweighting takes place. We also compared suppression ratios calculated  
 233 on Fourier components for the full trial, and found no significant effects of autism on suppression strength.  
 234 For Experiment 1 we assessed the first and second harmonics separately, but also found no AQ-related  
 235 differences. We therefore conclude that autism/AQ score is not associated with normalization reweighting, or  
 236 the strength of suppression more generally.

## 237 5 Discussion

238 We found evidence of dynamic normalization reweighting across three separate datasets. Suppression increased  
 239 significantly during the first 2-5 seconds of stimulus presentation, though with some variation across temporal  
 240 frequency. Reweighting had a similar timecourse for monocular and dichoptic stimulus presentation, and  
 241 was apparent as early as V1. We did not find compelling differences associated with autism, or high vs  
 242 low autistic traits. In the remainder of this section we will discuss possible explanations for temporal  
 243 frequency differences, evidence for inhibitory differences in autism, and more general implications of dynamic  
 244 normalization reweighting.

245 One important question is whether the dynamic increase in suppression can be explained by the stimulus onset  
 246 transient. This is a possibility that cannot be ruled out for some of our data. For example, the steep increase  
 247 in suppression in Figure 2f has a similar timecourse to the onset transient in Figure 2d. However, there are  
 248 also counterexamples where suppression continues to increase well beyond the first 1 second of stimulus  
 249 presentation (e.g. Figure 2e). It is currently unclear why there appear to be such substantial differences  
 250 between temporal frequency conditions, especially with such similar frequencies (5 and 7Hz). However the  
 251 differences are relatively consistent across experiments. For example, 5Hz flicker produces a more gradual  
 252 increase in suppression across all three data sets, compared with 7Hz flicker. These differences may be a  
 253 consequence of visual channels with different temporal tuning interacting with the stimulation frequency, as  
 254 well as any nonlinearities that govern suppression. Or there could be an asymmetry, whereby the relative  
 255 temporal frequency between the two stimulus components affects the character of suppression (Liza and Ray,  
 256 2022). We hope to be able to model these effects in the future, for example by using dynamic models of early  
 257 vision that incorporate time-lagged gain control (e.g. Zhou et al., 2019).

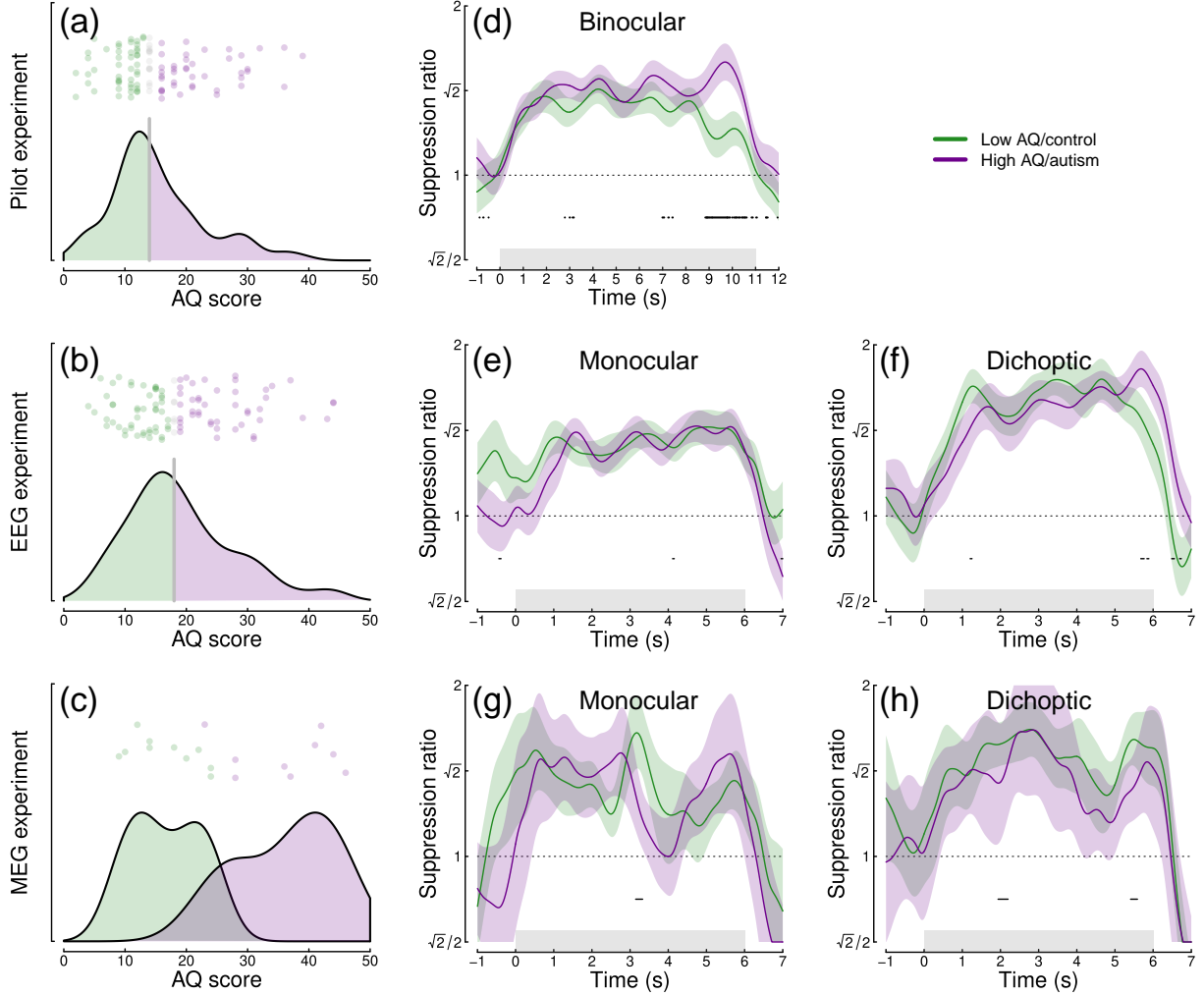


Figure 4: Analysis of the effect of autistic traits on normalization reweighting. Panels (a-c) show distributions of AQ scores across the three data sets. Panels (d-h) show timecourses of suppression averaged across stimulation frequency, and split by AQ score (d-f) or autism status (g, h). Panels (d,e,g) are for binocular or monocular presentation, and panels (f,h) are for dichoptic presentation. Shaded regions in panels (d-h) indicate  $\pm 1\text{SE}$  across participants, and black points at  $y = 0.8$  indicate significant differences between groups.

258 We did not observe clear differences in the timecourse between monocular and dichoptic suppression. This is  
259 important, because the dichoptic arrangement bypasses early stages of processing before the cortex (e.g. the  
260 retina and lateral geniculate nucleus). It suggests that the dynamic increases in suppression occur in the  
261 cortex, consistent with our MEG data that find evidence of reweighting in V1 (see Fig 3), and with previous  
262 neurophysiological work (Aschner et al., 2018). It is currently unclear whether these effects originate in V1, or  
263 might involve feedback from higher areas. The similarity between monocular and dichoptic effects also differs  
264 from work on adaptation to individual mask components. In both physiological (Li et al., 2005; Sengpiel and  
265 Vorobyov, 2005) and psychophysical (Baker et al., 2007) paradigms, adapting to a dichoptic mask reduces  
266 its potency, whereas adapting to a monocular mask has little or no effect. Normalization reweighting offers  
267 an explanation for why monocular masks presented in isolation do not adapt: if suppressive weights are  
268 determined by co-occurrence of stimuli, presentation of an isolated mask will have little effect. However  
269 this cannot explain the dichoptic adaptation effects without invoking additional binocular processes, such as  
270 competition between summing and differencing channels (e.g. May et al., 2012).

271 The relationship between normalization reweighting and other forms of visual plasticity is currently unclear.  
272 One phenomenon that might be closely related to our dichoptic effect is the change in interocular suppression  
273 that occurs when one eye is patched for a period of time (Lunghi et al., 2011). In the patching paradigm,  
274 the inputs to the two eyes are uncorrelated while one eye is patched, which the normalization reweighting  
275 model predicts should reduce suppression between the eyes. Most studies using patching have focussed on  
276 the resulting imbalance between the patched and non-patched eye, in which the patched eye contributes more  
277 to binocular single vision than the non-patched eye. In principle this could be due to increased suppression of  
278 the non-patched eye (inconsistent with normalization reweighting), or reduced suppression of the patched eye  
279 (consistent with normalization reweighting). It is difficult to distinguish these possibilities using paradigms  
280 that assess the balance between the two eyes, such as the binocular rivalry paradigm from the original Lunghi  
281 et al. (2011) study. However subsequent work has shown that patching increases the patched eye's response  
282 (Zhou et al., 2015), and reduces both dichoptic masking (Baldwin and Hess, 2018) and levels of the inhibitory  
283 neurotransmitter GABA (Lunghi et al., 2015). All of these findings are consistent with a reweighting account.

284 Autism is composed of a set of heterogenous symptoms and characteristics, and normalization reweighting  
285 may have a more specific relationship to some aspects of autism, rather than autism per se. For this reason,  
286 we also examined relationships with the sensory perception quotient (SPQ) to examine whether sensory  
287 experiences specifically were related to normalization reweighting. SPQ scores showed significant negative  
288 correlation with AQ for the data sets from Experiments 2 and 3 (EEG data,  $r = -0.35$ ,  $p < 0.001$ ; MEG data,  
289  $r = -0.57$ ,  $p = 0.011$ ) with effect sizes comparable to those reported previously (Tavassoli et al., 2014). We also  
290 conducted an exploratory analysis of the EEG data from Experiment 2, splitting participants by SPQ instead  
291 of AQ. However this analysis did not reveal any convincing differences in normalization reweighting either.  
292 Our preregistration also proposed to replicate our earlier finding of a reduced second harmonic response in  
293 participants with autism/high AQ scores. However the changes to the experimental design greatly reduced  
294 the second harmonic response in both experiments, such that it could not be observed reliably (see Figures  
295 2b and 3b). We were therefore not confident in conducting this analysis. We suspect that the increase in  
296 spatial frequency from 0.5 c/deg in the Vilidaite et al. (2018) study to 2 c/deg here is most likely responsible  
297 for the dramatically reduced second harmonic response.

298 The idea that the dynamic balance of inhibition and excitation might be different in autism (Rosenberg  
299 et al., 2015; Rubenstein and Merzenich, 2003) has compelling face validity. For example, individuals with  
300 autism often report difficulties with changes in their sensory environment, which might be due to gain control  
301 processes failing to adapt appropriately. Indeed, there is experimental evidence of reduced adaptation across  
302 various domains (Pellicano et al., 2007; Turi et al., 2015), which is predicted by some autism models (Pellicano  
303 and Burr, 2012). However this appears not to extend to changes in normalization reweighting, despite the  
304 link between reweighting and adaptation (Westrick et al., 2016).

## 305 5.1 Conclusions

306 We investigated the timecourse of normalization reweighting across three datasets, with a total of 220  
307 participants. We found clear evidence that suppression increases during the first 2–5 seconds of stimulus  
308 presentation, though there were differences across frequency that are currently unexplained. We did not

309 find evidence of autism-related differences in either the magnitude or timecourse of suppression. Our results  
310 support an emerging theory that suppression is a dynamic process that allows sensory systems to recalibrate  
311 according to their recent history.

## 312 6 Acknowledgements

313 Supported by BBSRC grant BB/V007580/1 awarded to DHB and ARW. We are grateful to all of the  
314 participants who took part in the experiments reported here.

## 315 References

- 316 Aschner A, Solomon SG, Landy MS, Heeger DJ, Kohn A. 2018. Temporal contingencies deter-  
317 mine whether adaptation strengthens or weakens normalization. *J Neurosci* **38**:10129–10142.  
318 doi:10.1523/JNEUROSCI.1131-18.2018
- 319 Baker DH. 2021. Statistical analysis of periodic data in neuroscience. *Neurons, Behavior, Data analysis, and*  
320 *Theory* **5**. doi:10.51628/001c.27680
- 321 Baker DH, Meese TS, Summers RJ. 2007. Psychophysical evidence for two routes to suppression before binocu-  
322 lar summation of signals in human vision. *Neuroscience* **146**:435–448. doi:10.1016/j.neuroscience.2007.01.030
- 323 Baldwin AS, Hess RF. 2018. The mechanism of short-term monocular deprivation is not simple: Separate  
324 effects on parallel and cross-oriented dichoptic masking. *Sci Rep* **8**:6191. doi:10.1038/s41598-018-24584-9
- 325 Baron-Cohen S, Wheelwright S, Skinner R, Martin J, Clubley E. 2001. The autism-spectrum quotient  
326 (AQ): Evidence from asperger syndrome/high-functioning autism, males and females, scientists and  
327 mathematicians. *J Autism Dev Disord* **31**:5–17. doi:10.1023/a:1005653411471
- 328 Blakemore C, Campbell FW. 1969. On the existence of neurones in the human visual system selectively sensi-  
329 tive to the orientation and size of retinal images. *J Physiol* **203**:237–60. doi:10.1113/jphysiol.1969.sp008862
- 330 Cannon MW, Fullenkamp SC. 1991. Spatial interactions in apparent contrast: Inhibitory effects among  
331 grating patterns of different spatial frequencies, spatial positions and orientations. *Vision Res* **31**:1985–98.  
332 doi:10.1016/0042-6989(91)90193-9
- 333 Carandini M, Heeger DJ. 2011. Normalization as a canonical neural computation. *Nature Reviews Neuro-  
334 science* **13**:51–62. doi:10.1038/nrn3136
- 335 Dale AM, Fischl B, Sereno MI. 1999. Cortical surface-based analysis. I. Segmentation and surface reconstruc-  
336 tion. *Neuroimage* **9**:179–94. doi:10.1006/nimg.1998.0395
- 337 Delorme A, Makeig S. 2004. EEGLAB: An open source toolbox for analysis of single-trial EEG dynamics includ-  
338 ing independent component analysis. *J Neurosci Methods* **134**:9–21. doi:10.1016/j.jneumeth.2003.10.009
- 339 Foley JM. 1994. Human luminance pattern-vision mechanisms: Masking experiments require a new model. *J  
340 Opt Soc Am A Opt Image Sci Vis* **11**:1710–9. doi:10.1364/josaa.11.001710
- 341 Foley JM, Chen CC. 1997. Analysis of the effect of pattern adaptation on pattern pedestal effects: A  
342 two-process model. *Vision Res* **37**:2779–88. doi:10.1016/s0042-6989(97)00081-3
- 343 Fonov V, Evans AC, Botteron K, Almlí CR, McKinstry RC, Collins DL, Brain Development Cooperative  
344 Group. 2011. Unbiased average age-appropriate atlases for pediatric studies. *Neuroimage* **54**:313–27.  
345 doi:10.1016/j.neuroimage.2010.07.033
- 346 Freeman TCB, Durand S, Kiper DC, Carandini M. 2002. Suppression without inhibition in visual cortex.  
347 *Neuron* **35**:759–71. doi:10.1016/s0896-6273(02)00819-x
- 348 Gibson JJ, Radner M. 1937. Adaptation, after-effect and contrast in the perception of tilted lines. I.  
349 Quantitative studies. *Journal of Experimental Psychology* **20**:453–467. doi:10.1037/h0059826
- 350 Greenlee MW, Georgeson MA, Magnussen S, Harris JP. 1991. The time course of adaptation to spatial  
351 contrast. *Vision Res* **31**:223–36. doi:10.1016/0042-6989(91)90113-j
- 352 Haak KV, Fast E, Bao M, Lee M, Engel SA. 2014. Four days of visual contrast deprivation reveals limits of  
353 neuronal adaptation. *Curr Biol* **24**:2575–9. doi:10.1016/j.cub.2014.09.027
- 354 Heeger DJ. 1992. Normalization of cell responses in cat striate cortex. *Vis Neurosci* **9**:181–97.  
355 doi:10.1017/s0952523800009640
- 356 Hoekstra RA, Vinkhuyzen AAE, Wheelwright S, Bartels M, Boomsma DI, Baron-Cohen S, Posthuma D,  
357 Sluis S van der. 2011. The construction and validation of an abridged version of the autism-spectrum

- 358 quotient (AQ-short). *J Autism Dev Disord* **41**:589–96. doi:10.1007/s10803-010-1073-0
- 359 Koh HC, Milne E, Dobkins K. 2010. Spatial contrast sensitivity in adolescents with autism spectrum disorders.  
360 *J Autism Dev Disord* **40**:978–87. doi:10.1007/s10803-010-0953-7
- 361 Kwon M, Legge GE, Fang F, Cheong AMY, He S. 2009. Adaptive changes in visual cortex following prolonged  
362 contrast reduction. *J Vis* **9**:20.1–16. doi:10.1167/9.2.20
- 363 Legge GE. 1979. Spatial frequency masking in human vision: Binocular interactions. *J Opt Soc Am* **69**:838–47.  
364 doi:10.1364/josa.69.000838
- 365 Li B, Peterson MR, Thompson JK, Duong T, Freeman RD. 2005. Cross-orientation suppression: Monoptic  
366 and dichoptic mechanisms are different. *J Neurophysiol* **94**:1645–50. doi:10.1152/jn.00203.2005
- 367 Liza K, Ray S. 2022. Local interactions between steady-state visually evoked potentials at nearby flickering  
368 frequencies. *J Neurosci* **42**:3965–3974. doi:10.1523/JNEUROSCI.0180-22.2022
- 369 Lunghi C, Burr DC, Morrone C. 2011. Brief periods of monocular deprivation disrupt ocular balance in  
370 human adult visual cortex. *Curr Biol* **21**:R538–9. doi:10.1016/j.cub.2011.06.004
- 371 Lunghi C, Emir UE, Morrone MC, Bridge H. 2015. Short-term monocular deprivation alters GABA in the  
372 adult human visual cortex. *Curr Biol* **25**:1496–501. doi:10.1016/j.cub.2015.04.021
- 373 MacLennan K, O'Brien S, Tavassoli T. 2022. In our own words: The complex sensory experiences of autistic  
374 adults. *J Autism Dev Disord* **52**:3061–3075. doi:10.1007/s10803-021-05186-3
- 375 Maris E, Oostenveld R. 2007. Nonparametric statistical testing of EEG- and MEG-data. *J Neurosci Methods*  
376 **164**:177–90. doi:10.1016/j.jneumeth.2007.03.024
- 377 Mather G, Pavan A, Campana G, Casco C. 2008. The motion aftereffect reloaded. *Trends Cogn Sci* **12**:481–7.  
378 doi:10.1016/j.tics.2008.09.002
- 379 May KA, Zhaoping L, Hibbard PB. 2012. Perceived direction of motion determined by adaptation to static  
380 binocular images. *Curr Biol* **22**:28–32. doi:10.1016/j.cub.2011.11.025
- 381 Meese TS, Baker DH. 2009. Cross-orientation masking is speed invariant between ocular pathways but speed  
382 dependent within them. *Journal of Vision* **9**:2. doi:10.1167/9.5.2
- 383 Pellicano E, Burr D. 2012. When the world becomes 'too real': A bayesian explanation of autistic perception.  
384 *Trends Cogn Sci* **16**:504–10. doi:10.1016/j.tics.2012.08.009
- 385 Pellicano E, Jeffery L, Burr D, Rhodes G. 2007. Abnormal adaptive face-coding mechanisms in children with  
386 autism spectrum disorder. *Curr Biol* **17**:1508–12. doi:10.1016/j.cub.2007.07.065
- 387 Petrov Y. 2005. Two distinct mechanisms of suppression in human vision. *Journal of Neuroscience* **25**:8704–  
388 8707. doi:10.1523/jneurosci.2871-05.2005
- 389 Rosenberg A, Patterson JS, Angelaki DE. 2015. A computational perspective on autism. *Proc Natl Acad Sci  
390 U S A* **112**:9158–65. doi:10.1073/pnas.1510583112
- 391 Rosenhall U, Nordin V, Sandström M, Ahlsén G, Gillberg C. 1999. Autism and hearing loss. *J Autism Dev  
392 Disord* **29**:349–57. doi:10.1023/a:1023022709710
- 393 Rubenstein JLR, Merzenich MM. 2003. Model of autism: Increased ratio of excitation/inhibition in key  
394 neural systems. *Genes Brain Behav* **2**:255–67. doi:10.1034/j.1601-183x.2003.00037.x
- 395 Sandhu TR, Reese G, Lawson RP. 2020. Preserved low-level visual gain control in autistic adults. *Wellcome  
396 Open Research* **4**. doi:10.12688/wellcomeopenres.15615.1
- 397 Schallmo M-P, Kolodny T, Kale AM, Millin R, Flevares AV, Edden RAE, Gerdts J, Bernier RA, Murray SO.  
398 2020. Weaker neural suppression in autism. *Nat Commun* **11**:2675. doi:10.1038/s41467-020-16495-z
- 399 Sengpiel F, Blakemore C. 1994. Interocular control of neuronal responsiveness in cat visual cortex. *Nature*  
400 **368**:847–50. doi:10.1038/368847a0
- 401 Sengpiel F, Vorobyov V. 2005. Intracortical origins of interocular suppression in the visual cortex. *J Neurosci*  
402 **25**:6394–400. doi:10.1523/JNEUROSCI.0862-05.2005
- 403 Simmons DR, Robertson AE, McKay LS, Toal E, McAleer P, Pollick FE. 2009. Vision in autism spectrum  
404 disorders. *Vision Research* **49**:2705–2739. doi:10.1016/j.visres.2009.08.005
- 405 Tadel F, Baillet S, Mosher JC, Pantazis D, Leahy RM. 2011. Brainstorm: A user-friendly application for  
406 MEG/EEG analysis. *Comput Intell Neurosci* **2011**:879716. doi:10.1155/2011/879716
- 407 Tavassoli T, Hoekstra RA, Baron-Cohen S. 2014. The sensory perception quotient (SPQ): Development  
408 and validation of a new sensory questionnaire for adults with and without autism. *Mol Autism* **5**:29.  
409 doi:10.1186/2040-2392-5-29
- 410 Tavassoli T, Latham K, Bach M, Dakin SC, Baron-Cohen S. 2011. Psychophysical measures of visual acuity  
411 in autism spectrum conditions. *Vision Research* **51**:1778–1780. doi:10.1016/j.visres.2011.06.004

- 412 Turi M, Burr DC, Igliozi R, Aagten-Murphy D, Muratori F, Pellicano E. 2015. Children with autism  
413 spectrum disorder show reduced adaptation to number. *Proc Natl Acad Sci U S A* **112**:7868–72.  
414 doi:10.1073/pnas.1504099112
- 415 Van de Cruys S, Vanmarcke S, Steyaert J, Wagemans J. 2018. Intact perceptual bias in autism contradicts  
416 the decreased normalization model. *Scientific Reports* **8**. doi:10.1038/s41598-018-31042-z
- 417 Van Veen BD, Drongelen W van, Yuchtman M, Suzuki A. 1997. Localization of brain electrical activi-  
418 ty via linearly constrained minimum variance spatial filtering. *IEEE Trans Biomed Eng* **44**:867–80.  
419 doi:10.1109/10.623056
- 420 Vilidaite G, Norcia AM, West RJH, Elliott CJH, Pei F, Wade AR, Baker DH. 2018. Autism sensory dysfunction  
421 in an evolutionarily conserved system. *Proc Biol Sci* **285**:20182255. doi:10.1098/rspb.2018.2255
- 422 Wang L, Mruczek REB, Arcaro MJ, Kastner S. 2015. Probabilistic maps of visual topography in human  
423 cortex. *Cereb Cortex* **25**:3911–31. doi:10.1093/cercor/bhu277
- 424 Webster MA. 2015. Visual adaptation. *Annu Rev Vis Sci* **1**:547–567. doi:10.1146/annurev-vision-082114-  
425 035509
- 426 Westrick ZM, Heeger DJ, Landy MS. 2016. Pattern adaptation and normalization reweighting. *Journal of  
427 Neuroscience* **36**:9805–9816. doi:10.1523/jneurosci.1067-16.2016
- 428 Yiltiz H, Heeger DJ, Landy MS. 2020. Contingent adaptation in masking and surround suppression. *Vision  
429 Res* **166**:72–80. doi:10.1016/j.visres.2019.11.004
- 430 Zhou J, Baker DH, Simard M, Saint-Amour D, Hess RF. 2015. Short-term monocular patching boosts the  
431 patched eye's response in visual cortex. *Restor Neurol Neurosci* **33**:381–7. doi:10.3233/RNN-140472
- 432 Zhou J, Benson NC, Kay K, Winawer J. 2019. Predicting neuronal dynamics with a delayed gain control  
433 model. *PLoS Comput Biol* **15**:e1007484. doi:10.1371/journal.pcbi.1007484